https://doi.org/10.1130/G51194.1

Manuscript received 22 February 2023

Revised manuscript received 30 June 2023

Manuscript accepted X Month 2023

Paul Kapp[ID]https://orcid.org/0000-0002-7173-9908

*pkapp@email.arizona.edu

CITATION: Kapp, P., et al., 2023, Laramide bulldozing of lithosphere beneath the Arizona transition zone, southwestern United States: Geology, v. XX, p. XXX–XXX, https://doi.org/10.1130/G51194.1

Printed in the USA

[1]Supplemental Material. Analytical methods, data tables and figures, and thermal modeling information. Please visit https://doi.org/10.1130/GEOL.S.XXXX to access the supplemental material, and contact editing@geosociety.org with any questions.

Laramide bulldozing of lithosphere beneath the Arizona transition zone, southwestern United States

Paul Kapp[1*], Gilby Jepson[2], Barbara Carrapa[1], Allen J. Schaen[1], John J.Y. He[1], and Jordan W. Wang[1]

[1]*Department of Geosciences, University of Arizona, Tucson, Arizona 85721, USA*

[2]*School of Geosciences, University of Oklahoma, Norman, Oklahoma 73019, USA*

ABSTRACT

The northwest-trending transition zone (TZ) in Arizona (southwestern United States) is an ~100-km-wide physiographic province that separates the relatively undeformed southwestern

DOI:10.1130/G51194.1

margin of the Colorado Plateau from the hyperextended Basin and Range province to the southwest. The TZ is widely depicted to have been a Late Cretaceous–Paleogene northeast-dipping erosional slope along which Proterozoic rocks were denuded but not significantly deformed. Our multi-method thermochronological study (biotite ^{40}Ar/^{39}Ar, zircon and apatite [U-Th-Sm]/He, and apatite fission track) of Proterozoic rocks in the Bradshaw Mountains of the west-central Arizona TZ reveals relatively rapid cooling (~10 °C/m.y.) from temperatures of >180 °C to <60 °C between ca. 70 and ca. 50 Ma. Given minimal ca. 70–50 Ma upper-crustal shortening in the TZ, we attribute cooling to exhumation driven by northeastward bulldozing of continental lower crust and mantle lithosphere beneath it by the Farallon flat slab. Bulldozing is consistent with contemporaneous (ca. 70–50 Ma) underplating and initial exhumation of Orocopia Schist to the southwest in western Arizona and Mesozoic garnet-clinopyroxenite xenoliths of possible Mojave batholith keel affinity in ca. 25 Ma TZ volcanic rocks.

INTRODUCTION

An outstanding question in tectonics is the extent to which flat-slab oceanic subduction beneath continental lithosphere can drive inboard translation and thickening of continental lower crust. The anomalously thick crust of the Rocky Mountain foreland and Great Plains has been attributed to inboard shearing of North American lithosphere by flat-slab subduction during the Laramide (ca. 85–40 Ma) orogeny (Bird, 1984). In the southwestern United States, very shallow Laramide flat-slab subduction is inferred to have juxtaposed subducted, mostly clastic sedimentary rocks (Orocopia and related schists; henceforth Orocopia Schist) at depths of ~35 km beneath continental crust over an inboard distance of ≥200 km (Fig. 1; Chapman, 2016; Jacobson et al., 2017; Seymour et al., 2018). This hypothesis requires preexisting continental lower crust and mantle lithosphere to have foundered into the mantle or been bulldozed inboard ahead of the leading hinge in the flat slab (Axen et al., 2018; Chapman et al., 2020a).

The transition zone (TZ) in Arizona is a topographically rugged physiographic province separating the southwestern Colorado Plateau from the Basin and Range province (Fig. 1). The TZ is transitional in the magnitude of Oligocene–Miocene extensional deformation, modern crustal thickness (decreasing southwestward across it from ~45 km to ~25 km), and mean elevation (Tork Qashqai et al., 2016). The western TZ exposes 1.8–1.6 Ga (meta)granitic and metasedimentary rocks, ca. 1.4 Ga plutons, and ca. 80–65 Ma tonalitic stocks (Fig. 2; DeWitt et al., 2008). Proterozoic rocks are buried in places by Neogene syn- to post-extensional sedimentary basins and volcanic rocks (DeWitt et al., 2008). The nonconformity between Proterozoic rocks and Paleozoic strata is exposed in the northern TZ and dips regionally <1°–2° to the northeast (Fig. 1). The TZ was not significantly shortened during Laramide orogenesis (Jenney and Reynolds, 1989) but became a proximal source of fluvial sandstone and conglomerate in northwestern Arizona by ca. 64 Ma (Fig. 1; Young and Hartman, 2014; Hill et al., 2016). Recent studies raise the possibility that continental lower crust and mantle lithosphere might have been bulldozed beneath the TZ during Laramide flat-slab subduction (e.g., Chapman et al., 2020a). The TZ is oriented nearly orthogonal to the ca. 80–50 Ma Farallon–North America relative plate convergence vector (Fig. 1) and within the corridor where a hypothesized oceanic plateau subducted beneath western North America (Livaccari et al., 1981; Saleeby, 2003). Integration of lithospheric strain rates back through time implicates a ≥55-km-thick crust within the TZ prior to Miocene extension (Bahadori et al., 2018). Igneous geochemical studies are also consistent with a previously thick TZ crust (~58 km at ca. 76 Ma; Chapman et al., 2020b). Garnet-clinopyroxenite xenoliths in ca. 25 Ma TZ volcanic rocks (Fig. 1) are interpreted to represent cumulates or residues that developed in situ during Laramide magmatism at depth (Erdman et al., 2016) or fragments of the mafic keel to the Mojave batholith that were bulldozed beneath the TZ (Chapman et al., 2020a; Rautela et al., 2020). Orocopia Schist exposed at Cemetery Ridge and the Plomosa Mountains (Fig. 1; Jacobson et al., 2017; Seymour et al., 2018) would have abutted the southwestern TZ prior to ~100 km of intervening Miocene northeast-southwest extension (Spencer and Reynolds, 1990**[[changed year to match Reference List]]**). If crustal thickening of the TZ by bulldozing did occur, it should have been active at least when Orocopia Schist was being emplaced beneath western Arizona at ca. 70–65 Ma (Chapman, 2016; Jacobson et al., 2017; Seymour et al., 2018) and might have induced erosion-driven exhumation as topographic relief was generated in the TZ. This timing prediction motivated our thermochronological study of the TZ.

PREVIOUS THERMOCHRONOLOGIC DATA

Thermochronological data record information about the timing of rock cooling below their respective closure temperature windows, which are broad but nominally ~250–400 °C for biotite $^{40}Ar/^{39}Ar$, ~200–240 °C for zircon fission track (ZFT), ~180 °C for zircon (U-Th-Sm)/He (ZHe), ~60–115 °C for apatite fission track (AFT), and ~60–80 °C for apatite (U-Th-Sm)/He (AHe) (Reiners et al., 2018, and references therein). Biotite K-Ar and $^{40}Ar/^{39}Ar$ apparent ages from Proterozoic TZ rocks are overwhelmingly Proterozoic (DeWitt et al., 2008, and references therein). The Mesozoic–Cenozoic thermal history of the TZ is roughly constrained from three AFT ± ZFT transects that span the Poachie, Bradshaw, and Mazatzal Mountains**[[Poachie Range and Bradshaw and Mazatzal Mountains (according to the USGS geographic names database, GNIS)? Check all instances of "Poachie"]]** (Fig. 2; Bryant et al., 1991; Foster et al., 1993). These studies showed that TZ rocks cooled during Cretaceous–Cenozoic time from temperatures of <120 °C near the Proterozoic unconformity to >200 °C at the deeper structural levels now exposed in the southwest. The Poachie Mountains experienced moderate rates of cooling between ca. 85 and 55 Ma (Bryant et al., 1991). Elsewhere in the TZ, most AFT samples exhibit bimodal track-length distributions that suggest initial cooling during the Laramide orogeny followed by ≤25 Ma cooling associated with extension (Foster et al., 1993). There are no published ZHe or AHe data from the TZ, but an AHe investigation of the southwesternmost margin of the Colorado Plateau suggests >1.5 km of Late Cretaceous sedimentary burial followed by exhumation between ca. 60 and 50 Ma (Flowers et al., 2008).

METHODS

Our new igneous zircon U-Pb and biotite $^{40}Ar/^{39}Ar$, ZHe, AFT, and AHe data from the approximately northwest-trending Bradshaw Mountains come from samples of five Proterozoic granitoids, one Late Cretaceous stock, and one modern river sand (Fig. 2) (see the Supplemental Material[1] for analytical methods, data tables, supplemental data figures, and thermal modeling information). The samples span a range-parallel distance of ~50 km and elevations ranging from 994 to 2212 m. To limit the effects of ≤25 Ma tectonic exhumation or sedimentary burial, we focused our sampling within interior parts of the range located farthest away from Neogene extensional faults and basins. The number of individual zircon crystals analyzed for each of the four ZHe samples is only two to four because of their low yield of suitable zircons; for these samples, we report their unweighted mean age and standard deviation. A larger number of individual apatite crystals (*n* = 7–8) were analyzed for each of the three AHe samples; for these, we report first quartile dates (FQDs), which have been shown to provide the most geologically meaningful information for relatively low-*n* and relatively fast-cooled samples with dispersed single age distributions, along with 1σ uncertainties quantified through non-parametric bootstrapping (He et al., 2021).

RESULTS

Proterozoic rocks in the Bradshaw Mountains are locally intruded by kilometer-scale Late Cretaceous stocks with previously determined biotite/hornblende**[[Replace slash with "and", "or", or "and/or" (or other appropriate wording)]]** K-Ar dates ranging from 76 to 64 Ma (Fig. 2; DeWitt et al., 2008, and references therein). The K-Ar dates are generally taken to approximate the timing of post-magmatic thermal equilibration, which occurs within a few million years for stocks emplaced at shallow crustal depths (McInnes et al., 2005). Supporting this assumption is the consistency between a newly determined U-Pb zircon mean crystallization age of 71.9 ± 0.9 Ma (2σ; *n* = 33 zircon laser spot ages; Fig. S1 in the Supplemental Material) for a tonalitic stock (sample A in Fig. 2) and a biotite K-Ar date of ca. 70 Ma from an adjacent stock (Fig. 2). Sample A yields single-grain AHe dates ranging from ca. 37 to 66 Ma with a FQD of 44 ± 4 Ma (Fig. 3A), suggesting that the stock remained at temperature >~60 °C for >20 m.y. after crystallization. Sample B of a foliated Proterozoic granite located <1 km from a stock with a hornblende K-Ar date of ca. 64 Ma yields a ZHe date of 66 ± 1 Ma (*n* = 3) (Figs. 2 and 3B). Sample C of a ca. 1.7 Ga granodiorite located <1 km from a stock with a biotite K-Ar date of ca. 65 Ma yields an AFT central age of 61 ± 4 Ma and strongly dispersed individual AHe dates with a FQD of 52 ± 26 Ma (Figs. 2 and 3A). Given their similarity to adjacent K-Ar dates, the ZHe and AFT dates from samples B and C likely reflect thermal perturbations associated with magmatism.

ZHe dates from northernmost sample D and southernmost sample E of Proterozoic granitoids are 50 ± 4 Ma (*n* = 3) and 54.9 ± 0.5 Ma (*n* = 2), respectively (Figs. 2 and 3B).

DOI:10.1130/G51194.1

Because these ZHe dates are too young to reflect post-magmatic thermal equilibration, they are interpreted to record cooling in response to erosion. Two $^{40}Ar/^{39}Ar$ incremental heating experiments on biotite (one single crystal, one 0.5 mg aliquot) from sample E yield overall similar and discordant age spectra that do not meet plateau criteria (Figs. S2 and S3). Apparent ages increase from ca. 30 to ca. 50 Ma during progressive degassing and are younger than the two individual ca. 55 Ma ZHe dates for the same sample. The most likely explanation for the anomalously young apparent ages is partial alteration of biotite to vermiculate**[[Do you mean "vermiculite"?]]** as determined using Raman spectroscopy (Fig. S4).

Two $^{40}Ar/^{39}Ar$ incremental heating experiments on biotite (one single crystal, one 1 mg aliquot) from easternmost sample F of a ca. 1.7 Ga granite (DeWitt et al., 2008) yield similarly shaped age spectra that range from ca. 0.8 Ga to ca. 1.4 Ga (Fig. S5). Omitting the initial ~7% $^{39}Ar_K$**[[Explain what the subscript "K" represents]]** from each experiment yields coeval inverse isochron ages of ca. 1.4 Ga with subatmospheric $^{40}Ar/^{36}Ar$ intercept values resulting from apparent Ar loss (Fig. S6). Sample F also yields a ZHe date of 64 ± 8 Ma (n = 4), an AFT central age of 53 ± 4 Ma, and an AHe FQD of 48 ± 8 Ma (Figs. 2 and 3). Inverse thermal history modeling using QTQt 5.7.0 (Gallagher, 2012) on samples C and F (see the Supplemental Material), integrating the AFT central age and single-grain age distribution, confined track-length distribution, thermal influence of the ca. 65 Ma stock on sample C, and ZHe and/or AHe single-grain dates, reveals an episode of accelerated cooling (~10 °C/m.y.) from ~150–200 °C to near-surface temperature between ca. 70 and 50 Ma (Fig. 3C).

Lastly, detrital AFT dates (n = 117) on sample G of modern Hassayampa River sand yield a unimodal distribution with a central age of 55.8 ± 1.4 Ma (Fig. 2; Fig. S7). The catchment area for sample G is only ~9 km^2 but located ~20 km to the northwest of sample F in a different

DOI:10.1130/G51194.1

catchment with an indistinguishable AFT central age of 53 ± 4 Ma, suggestive of a similar and regional low-temperature cooling history for the central Bradshaw Mountains.

DISCUSSION AND CONCLUSIONS

Our thermochronologic data from the Bradshaw Mountains suggest rapid (~10 °C/m.y.) cooling between ca. 70 and 50 Ma. Initial cooling at ca. 70–65 Ma could reflect post-magmatic thermal equilibration, but most of the subsequent cooling is attributed to erosion. Both the Poachie Mountains to the west and the southwesternmost Colorado Plateau to the northeast, where Late Cretaceous intrusions are absent, experienced cooling between ca. 85–80 Ma and ca. 50 Ma (Bryant et al., 1991; Flowers et al., 2008; Fig. 3C). The Basin and Range province to the southwest also records widespread ca. 80–50 Ma cooling prior to Miocene core complex development (Fig. 2; e.g., Knapp and Heizler, 1990; Wong et al., 2023). The Orocopia Schist, Maria fold-thrust belt, a narrow northwest-trending belt of metamorphic core complexes between Phoenix (Arizona) and southeastern California, garnet-clinopyroxenite xenolith localities, and the oldest (Paleocene) Rim**[[Explain what “Rim” refers to (check all instances for clarity)]]** gravels in northwestern Arizona are all exposed along the trajectory where the Farallon flat slab plowed into the southwestern Cordilleran orogen (Fig. 1). We present a tentative regional tectonic history that attempts to link these elements with the evolution of the TZ.

In contrast to the TZ, Late Cretaceous shortening is significant in southeastern California and western Arizona as manifested by the basement-involved but thin-skinned-style and ductile Maria fold-thrust belt (Fig. 1; Reynolds et al., 1986; Hamilton, 1987; Spencer and Reynolds, 1990; Boettcher et al., 2002).Thrusts and folds generally verge toward the south-southwest, in contrast to the east-vergent Sevier thrust belt to the north (Fig. 1), and were active between ca. 90 and 70 Ma (Reynolds et al., 1986; Knapp and Heizler, 1990; Boettcher et al., 2002). Hence, the

DOI:10.1130/G51194.1

Maria fold-thrust belt could have fed crust in the footwall of its décollement beneath the TZ (Fig. 4A). Underthrusting could explain ca. 85–70 Ma exhumation in the Poachie Mountains and thick crust in the TZ by ca. 76 Ma (Chapman et al., 2020b).

The beginning of flat-slab subduction near the trench at ca. 90 Ma (Chapman, 2016) might have accelerated shortening within the Maria fold-thrust belt, ~~while~~ whereas the passage of the buoyant flat slab and underplating of Orocopia Schist beneath the continental margin may have led to its ca. 70–50 Ma extensional reactivation (e.g., Boettcher et al., 2002; Wong et al., 2023). Ca. 70–50 Ma cooling of the TZ, perhaps driven by inboard bulldozing of lithosphere beneath it, was coeval with initial river incision and Rim gravel deposition in northwestern Arizona (Young and Hartman, 2014; Hill et al., 2016) (Fig. 4B). Eclogite xenoliths in the Navajo volcanic field**[[Briefly describe where this is located relative to the study area]]** suggest that the top of the Farallon slab was located at a depth of ~120 km beneath the Four Corners region**[[Unclear whether this is a reference that would be widely understood by an international audience. Perhaps give geographical context – e.g., "(northeastern corner of Arizona)"?]]** (Hernández-Uribe and Palin, 2019, and references therein), implicating a hinge in the flat slab. A logical place for a hinge to have formed is where the flat slab first encountered stronger lithosphere as it translated inboard. Lithosphere to the southwest of the TZ was weakened by Mesozoic magmatism, lithospheric thinning during Border**[[Explain what "Border" refers to]]** rift development, and Late Cretaceous crustal shortening and anatexis (Jenney and Reynolds, 1989), whereas Colorado Plateau lithosphere experienced none of this. The location of the hinge in the flat slab at the TZ can also explain why bulldozed lithosphere thickened preferentially beneath it (Fig. 4B).

DOI:10.1130/G51194.1

Beginning at ca. 25 Ma, ductile crust extruded to the southwest from beneath the TZ in the footwalls of large-displacement detachment faults (Spencer and Reynolds, 1989; Bryant et al., 1991), drainage reversed from northeastward to southwestward across the TZ (Anderson et al., 2021; Potochnik et al., 2022), and volcanism became more widespread (Fig. 4C). Extensional collapse is attributed to foundering of the Farallon slab and dense bulldozed lithosphere and was directed southwestward by the buoyancy of the TZ crustal root (Fig. 4C; Chapman et al., 2020a).

ACKNOWLEDGMENTS

This research was supported by U.S. National Science Foundation (NSF) grant EAR-2048656. The Arizona LaserChron Center and Noble Gas Laboratory (University of Arizona) are funded by NSF grants EAR-1649254 and EAR-182692.**[[Is this grant number missing a digit?]]** We thank D. Alberts and J. Headley for laboratory assistance and A. Chapman, C. Jacobson, and N. Seymour for constructive reviews.

REFERENCES CITED

Anderson, J.C., Karlstrom, K.E., and Heizler, M.T., 2021, Neogene drainage reversal and Colorado Plateau uplift in the Salt River area, Arizona, USA: Geomorphology, v. 395, https://doi.org/10.1016/j.geomorph.2021.107964.

Axen, G.J., van Wijk, J.W., and Currie, C.A., 2018, Basal continental mantle lithosphere displaced by flat-slab subduction: Nature Geoscience, v. 11, p. 961–964, https://doi.org/10.1038/s41561-018-0263-9.

Bahadori, A., Holt, W.E., and Rasbury, E.T., 2018, Reconstruction modeling of crustal thickness and paleotopography of western North America since 36 Ma: Geosphere, v. 14, p. 1207–1231, https://doi.org/10.1130/GES01604.1.

Bird, P., 1984, Laramide crustal thickening event in the Rocky Mountain foreland and Great Plains: Tectonics, v. 3, p. 741–758, https://doi.org/10.1029/TC003i007p00741.

Boettcher, S.S., Mosher, S., and Tosdal, R.M., 2002, Structural and tectonic evolution of Mesozoic basement-involved fold nappes and thrust faults in the Dome Rock Mountains, Arizona, *in* Barth, A., ed., Contributions to Crustal Evolution of the Southwestern United States: Geological Society of America Special Paper 365, p. 73–97, https://doi.org/10.1130/0-8137-2365-5.73.

Bryant, B., Naeser, C.W., and Fryxell, J.E., 1991, Implications of low-temperature cooling history on a transect across the Colorado Plateau–Basin and Range boundary, west central Arizona: Journal of Geophysical Research, v. 96, p. 12,375–12,388, https://doi.org/10.1029/90JB02027.

Chapman, A.D., 2016, The Pelona-Orocopia-Rand and related schists of southern California: A review of the best-known archive of shallow subduction on the planet: International Geology Review, v. 59, p. 664–701, https://doi.org/10.1080/00206814.2016.1230836.

Chapman, A.D., Rautela, O., Shields, J., Ducea, M.N., and Saleeby, J., 2020a, Fate of the lower lithosphere during shallow-angle subduction: The Laramide example: GSA Today, v. 30, no. 1, p. 4–10, https://doi.org/10.1130/GSATG412A.1.

Chapman, J.B., Greig, R., and Haxel, G.B., 2020b, Geochemical evidence for an orogenic plateau in the southern U.S. and northern Mexican Cordillera during the Laramide orogeny: Geology, v. 48, p. 164–168, https://doi.org/10.1130/G47117.1.

DeWitt, E., Langenheim, V.E., Force, E., Vance, R.K., Lindberg, P.A., and Driscoll, R.L., 2008, Geologic map of the Prescott National Forest and the headwaters of the Verde River, Yavapai and Coconino Counties, Arizona: U.S. Geological Survey Scientific Investigations Map 2996, scale 1:100,000, 100 p., https://doi.org/10.3133/sim2996.

Erdman, M.E., Lee, C.-T.A., Levander, A., and Jiang, H.H., 2016, Role of arc magmatism and lower crustal foundering in controlling elevation history of the Nevadaplano and Colorado Plateau: A case study of pyroxenitic lower crust from central Arizona, USA: Earth and Planetary Science Letters, v. 439, p. 48–57, https://doi.org/10.1016/j.epsl.2016.01.032.

Flowers, R.M., Wernicke, B.P., and Farley, K.A., 2008, Unroofing, incision, and uplift history of the southwestern Colorado Plateau from apatite (U-Th)/He thermochronometry: Geological Society of America Bulletin, v. 120, p. 571–587, https://doi.org/10.1130/B26231.1.

Foster, D.A., Gleadow, A.J.W., Reynolds, S.J., and Fitzgerald, P.G., 1993, Denudation of metamorphic core complexes and the reconstruction of the transition zone, west central Arizona: Constraints from apatite fission track thermochronology: Journal of Geophysical Research, v. 98, p. 2167–2185, https://doi.org/10.1029/92JB02407.

Gallagher, K., 2012, Transdimensional inverse thermal history modeling for quantitative thermochronology: Journal of Geophysical Research, v. 117, B02408, https://doi.org/10.1029/2011JB008825.

Hamilton, W.B., 1987, Mesozoic geology and tectonics of the Big Maria Mountains region, southeastern California, *in* Dickinson, W.R., and Klute, M.A., eds., Mesozoic Rocks of Southern Arizona and Adjacent Areas: Arizona Geological Society Digest 18, p. 33–47.

He, J., Thomson, S.N., Reiners, P.W., Hemming, S.R., and Licht, K.J., 2021, Rapid erosion of the central Transantarctic Mountains at the Eocene-Oligocene transition: Evidence from skewed (U-Th)/He date distributions near Beardmore Glacier: Earth and Planetary Science Letters, v. 567, https://doi.org/10.1016/j.epsl.2021.117009.

Hernández-Uribe, D., and Palin, R.M., 2019, Catastrophic shear-removal of subcontinental lithospheric mantle beneath the Colorado Plateau by the subducted Farallon slab: Scientific Reports, v. 9, 8153, https://doi.org/10.1038/s41598-019-44628-y.

Hill, C.A., Polyak, V.J., Asmerom, Y., and Provencio, P.P., 2016, Constraints on a Late Cretaceous uplift, denudation, and incision of the Grand Canyon region, southwestern Colorado Plateau, USA, from U-Pb dating of lacustrine limestone: Tectonics, v. 35, p. 896–906, https://doi.org/10.1002/2016TC004166.

Jacobson, C.E., Hourigan, J.K., Haxel, G.B., and Grove, M., 2017, Extreme latest Cretaceous–Paleogene low-angle subduction: Zircon ages from Orocopia Schist at Cemetery Ridge, southwestern Arizona, USA: Geology, v. 45, p. 951–954, https://doi.org/10.1130/G39278.1.

Jenney, J.P., and Reynolds, S.J., eds., 1989, Geologic Evolution of Arizona: Arizona Geological Society Digest 17, 866 p.

Knapp, J.H., and Heizler, M.T., 1990, Thermal history of crystalline nappes of the Maria fold and thrust belt, west central Arizona: Journal of Geophysical Research, v. 95, p. 20,049–20,073, https://doi.org/10.1029/JB095iB12p20049.

Livaccari, R.F., Burke, K., and Sengor, A.M.C., 1981, Was the Laramide orogeny related to subduction of an oceanic plateau?: Nature, v. 289, p. 276–278, https://doi.org/10.1038/289276a0.

McInnes, B.I.A., Evans, N.J., Fu, F.Q., and Garvin, S., 2005, Application of thermochronology to hydrothermal ore deposits: Reviews in Mineralogy and Geochemistry, v. 58, p. 467–498, https://doi.org/10.2138/rmg.2005.58.18.

Potochnik, A.R., Faulds, J.E., and Reynolds, S.R., 2022, Cenozoic drainage reversal on the southern margin of the Colorado Plateau, east-central Arizona, USA: Geomorphology, v. 411, https://doi.org/10.1016/j.geomorph.2022.108286.

Prior, M.G., Stockli, D.F., and Singleton, J.S., 2016, Miocene slip history of the Eagle Eye detachment fault, Harquahala Mountains metamorphic core complex, west-central Arizona: Tectonics, v. 35, p. 1913–1934, https://doi.org/10.1002/2016TC004241.

Rautela, O., Chapman, A.D., Shields, J.E., Ducea, M.N., Lee, C.-T., Jiang, H.H., and Saleeby, J., 2020, In search for the missing arc root of the Southern California Batholith: P-T-t evolution of upper mantle xenoliths of the Colorado Plateau Transition Zone: Earth and Planetary Science Letters, v. 547, https://doi.org/10.1016/j.epsl.2020.116447.

Reiners, P.W., Carlson, R.W., Renne, P.R., Cooper, K.M., Granger, D.E., McLean, N.M., and Schoene, B., 2018, Geochronology and Thermochronology: Oxford, John Wiley and Sons Ltd, 464 p.

Reynolds, S.J., Spencer, J.E., Richard, S.M., and Laubach, S.E., 1986, Mesozoic structures in west-central Arizona, *in* Beatty, B., and Wilkinson, P.A.K., eds., Frontiers in Geology and Ore Deposits of Arizona and the Southwest: Arizona Geological Society Digest 16, p. 35–51.

Saleeby, J., 2003, Segmentation of the Laramide Slab—Evidence from the southern Sierra Nevada region: Geological Society of America Bulletin, v. 115, p. 655–668, https://doi.org/10.1130/0016-7606(2003)115<0655:SOTLSF>2.0.CO;2.

Seymour, N.M., Strickland, E.D., Singleton, J.S., Stockli, D.F., and Wong, M.S., 2018, Laramide subduction and metamorphism of the Orocopia Schist, northern Plomosa Mountains, west-central Arizona: Insights from zircon U-Pb geochronology: Geology, v. 46, p. 847–850, https://doi.org/10.1130/G45059.1.

Singleton, J.S., Stockli, D.F., Gans, P.B., and Prior, M.G., 2014, Timing, rate, and magnitude of slip on the Buckskin-Rawhide detachment fault, west central Arizona: Tectonics, v. 33, p. 1596–1615, https://doi.org/10.1002/2013TC003517.

Spencer, J.E., and Reynolds, S.J., 1990, Relationship between Mesozoic and Cenozoic tectonic features in west central Arizona and adjacent southeastern California: Journal of Geophysical Research, v. 95, p. 539–555, https://doi.org/10.1029/JB095iB01p00539.

Tork Qashqai, M., Afonso, J.C., and Yang, Y.J., 2016, The crustal structure of the Arizona Transition Zone and southern Colorado Plateau from multiobservable probabilistic inversion: Geochemistry, Geophysics, Geosystems, v. 17, p. 4308–4332, https://doi.org/10.1002/2016GC006463.

Wong, M.S., Singleton, J.S., Seymour, N.M., Gans, P.B., and Wrobel, A.J., 2023, Late Cretaceous–early Paleogene extensional ancestry of the Harcuvar and Buckskin-Rawhide metamorphic core complexes, western Arizona: Tectonics, v. 42, https://doi.org/10.1029/2022TC007656.

Young, R.A., and Hartman, J.H., 2014, Paleogene rim gravel of Arizona: Age and significance of the Music Mountain Formation: Geosphere, v. 10, p. 870–891, https://doi.org/10.1130/GES00971.1.

Figure 1. Late Cretaceous–Eocene reconstruction of the American Southwest Cordillera**[[Do you mean, e.g., “North American Cordillera in the southwestern United States”?]]** and major tectonic elements (modified after Chapman, 2016, and Saleeby, 2003). CR—Cemetery Ridge; Pl—Plomosa Mountains; X-Pz—nonconformity between Proterozoic rocks and Paleozoic

strata.**[[In the figure, include labeled latitude/longitude markings if applicable; make instances of “plate” and “zone” lowercase (and “transitional” unless first letter of each text label gets capitalized); on ages, change instances of “~” to “ca.” (leave as “~” on other types of measurements)]]**

Figure 2. Shaded relief map (www.geomapapp.org) of west-central Arizona summarizing previous and new (samples A–G) thermochronologic results. Low-temperature thermochronometric dates from metamorphic core complexes (MCCs) to the southwest of the transition zone (TZ) are mostly Miocene while those in the hanging wall include older dates overlapping with those from the TZ (e.g., Bryant et al., 1991; Foster et al., 1993; Singleton et al., 2014; Prior et al., 2016). ZFT—zircon fission track; ZHe—zircon helium; AFT—apatite fission track; AHe—apatite helium.**[[In the figure, should “Poachie Mts.” be “Poachie Range” (see query in text)?; make instances of “zone” lowercase (and “transitional” unless the first letter of each label gets capitalized); capitalize “Unconformity”; on ages, change instances of “~” to “ca.”]]**

Figure 3. (A) Individual (black circles), median (black horizontal lines and lettering), and first quartile apatite helium (AHe) dates (red horizontal lines and lettering); one >160 Ma date from sample C is excluded.**[[Explain what the “I” bars represent]]** (B) Zircon helium (ZHe) dates versus effective uranium concentration (eU).**[[Explain what the ages at the tops of the panels represent; explain what the error bars represent]]** (C) Thermal history models performed in QTQt 5.7.0 (Gallagher, 2012) of samples C and F (blue lines with gray shading) and southwestern Colorado Plateau samples CP-06-01, CP-06-19, and CP-06-20 of Flowers et al. (2008). **[[Explain what is represented by the gray shading (for the samples of this study) and the dashed black lines (for the SW Colorado Plateau samples)]]** Poachie Mountains

samples (Bryant et al., 1991) were not modeled because of insufficient single-grain data.**[[Explain what the error bars on the Poachie samples represent]]** Thermal history modeling inputs and fits are provided in Supplemental Material (see footnote 1). AHe PRZ—apatite helium partial retention zone; AFT PAZ—apatite fission-track partial annealing zone; ZHe PRZ—zircon helium partial retention zone; ZFT—zircon fission track.**[[In the figure, panel C, change "Bradshaw" to "Bradshaw Mountains", and "Poachie" to "Poachie Mountains" or "Poachie Range" (see query in text re: Mountains vs. Range); in the horizontal-axis description, would "Age" be a more accurate term than "Time"?]]**

Figure 4. Cross-sectional interpretations of Late Cretaceous to Neogene tectonic evolution of western Arizona. (A) Maria fold-thrust belt shortening led to northeastward underthrusting of crust beneath the transition zone (TZ). MMT—Mule Mountains thrust; Pz-Mz—Paleozoic–Mesozoic. (B) Flat-slab oceanic subduction emplaced Orocopia Schist beneath western Arizona and bulldozed continental lower crust and mantle lithosphere beneath the TZ. (C) Foundering of Farallon flat slab and dense bulldozed lithosphere resulted in volcanism, extensional collapse, and drainage reversal across the TZ.**[[Explain what "Rim" refers to]] [[In the figure, label the vertical axes with a text description and units of measure in parentheses – e.g., "Depth (km)"; make "zone" lowercase; on ages, change instances of "~" to "ca.". In panel A, capitalize "Basin"]]**

Figure 1 Kapp et al.

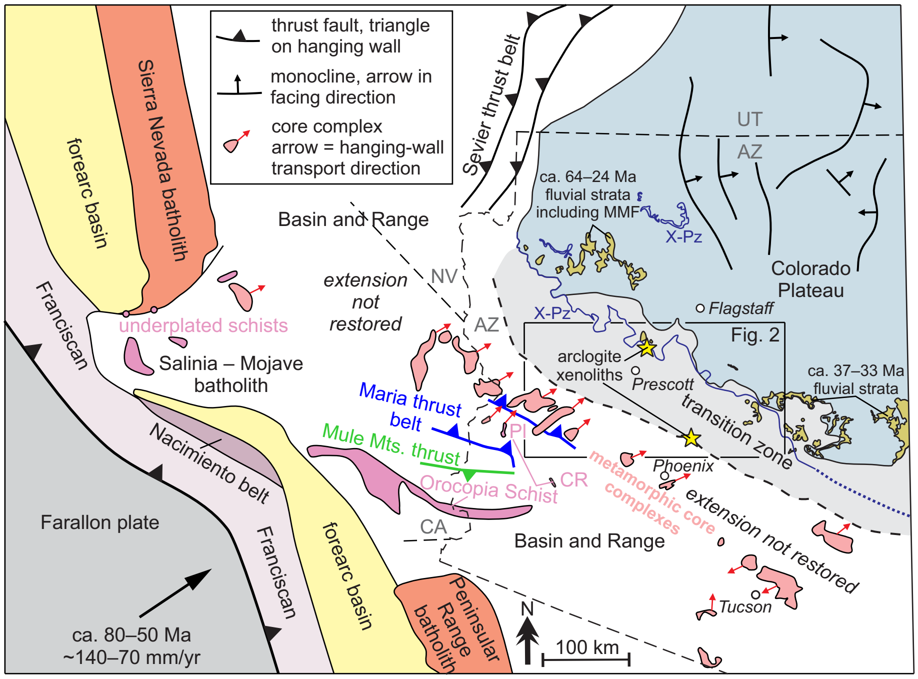

Figure 2 Kapp et al.

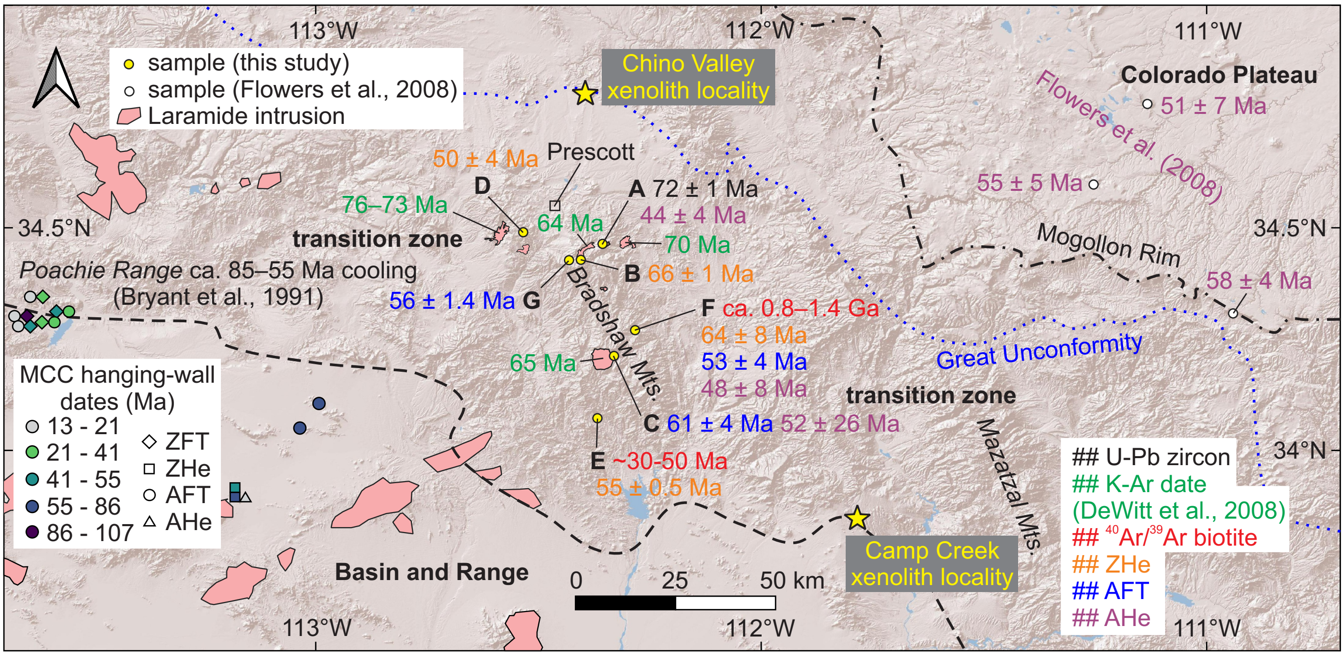

Figure 3 Kapp et al.

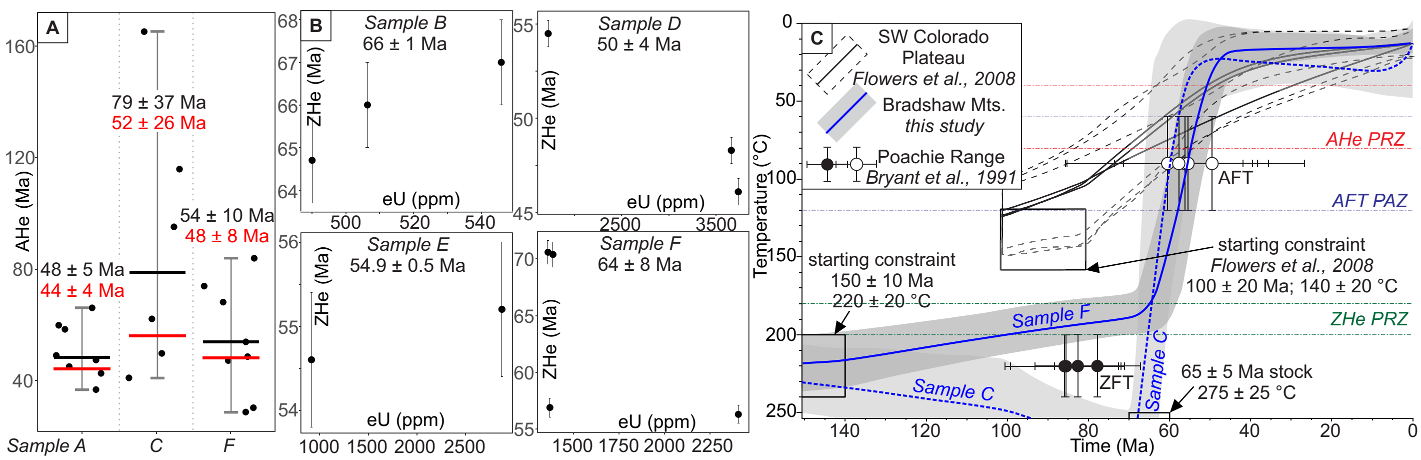

Figure 4 Kapp et al.